Geophys. J. Int. (1997) **129,** 669–680

Reflection and transmission of *qP–qS* plane waves at a plane boundary between viscoelastic transversely isotropic media

José M. Carcione
Osservatorio Geofisico Sperimentale, PO Box 2011 *Opicina,* 34016 *Trieste, Italy. E-mail: carcione@gems755.ogs.trieste.it*

Accepted 1997 February 11. Received 1997 February 10; in original form 1996 March 25

SUMMARY

We consider the problem of reflection and transmission in two viscoelastic transversely isotropic (VTI) media in contact, with the symmetry axis of each medium perpendicular to the interface. The problem is investigated by means of a plane-wave analysis and a numerical simulation experiment. For an incident homogeneous wave, the reflected wave is of the same type and is also homogeneous, while the other waves are inhomogeneous, that is, equiphase planes do not coincide with equiamplitude planes. If the transmission medium is elastic, the refracted waves are inhomogeneous of the elastic type, that is, the attenuation vectors are perpendicular to the respective Umov–Poynting vectors (energy direction). On the other hand, if the incidence medium is elastic and the transmission medium anelastic, the attenuation vectors of the transmitted waves are perpendicular to the interface.

The angle between the attenuation and the real slowness vectors may exceed 90°, but the angle between the attenuation and the Umov–Poynting vectors is always less than 90°. As in the anisotropic case, energy flow parallel to the interface is the criterion for obtaining a critical angle, which exists only in rare instances in viscoelastic media. In fact, for this particular example, the transmitted flux of the quasi-compressional wave is always greater than zero. To balance energy flux it is necessary to consider the interference fluxes between the different waves (these fluxes vanish in the elastic case). The relevant physical phenomena are related to the energy flow direction (Umov–Poynting vector) rather than to the propagation direction (real slowness vector).

The simulation experiment gives the particle velocity fields caused by a mean stress source. The results are in good agreement with the plane-wave analysis, despite the fact that only a qualitative comparison can be performed. The presence of the conical wave, which cannot be explained with a plane analysis, indicates that, in spite of the absence of a critical angle, some of the refracted energy disturbs the interface.

Key words: anisotropy, attenuation, modelling, reflection, refraction.

INTRODUCTION

The problem of reflection and refraction at an interface between two anelastic transversely isotropic media whose z-crystallographic axes are perpendicular to the interface has a practical application in the exploration for hydrocarbon reservoirs by seismic waves. The interface may separate two finely layered formations whose contact plane is parallel to the stratification. Anelastic rheology models the different attenuation mechanisms due to the presence of cracks and fluid saturation.

To our knowledge, the viscoelastic problem has been addressed only in the isotropic case. For instance, Cooper (1967), Buchen (1971) and Schoenberg (1971) found that *inhomogeneous viscoelastic wavefields* are required to satisfy the boundary conditions. Borcherdt, Glassmoyer & Wennerberg (1986) presented theoretical and experimental results and cited most of the relevant work carried out by R. Borcherdt on the subject. E. Krebes also contributed to the solution of the problem, mainly in connection with ray tracing in viscoelastic media (e.g. Krebes & Slawinski 1991). A comprehensive review of the problem is given in Caviglia & Morro (1992). The most relevant difference from the elastic case is the presence of inhomogeneous waves which have a body-wave character, in contrast to the inhomogeneous waves of the *elastic type*, which propagate along interfaces. For viscoelastic inhomogeneous waves the angle between the propagation and attenuation vectors is strictly less than 90°, unlike elastic inhomogeneous waves. Depending on the inhomogeneity of the wave, its behaviour (e.g. phase velocity,

attenuation, particle motion) may differ substantially from that of elastic waves.

Analyses of the elastic anisotropic problem can be found in Musgrave (1960), Henneke (1971), Daley & Hron (1977), Keith & Crampin (1977), Rokhlin, Bolland & Adler (1986) and Graebner (1992). In the anisotropic case, it is very important to study the problem in terms of energy flow rather than amplitude, since the energy flow direction in general does not coincide with the propagation (wave-vector) direction. Critical angles occur when the ray (energy flow) direction is parallel to the interface.

DIFFERENTIAL EQUATIONS FOR HETEROGENEOUS MEDIA

The time-domain equations for propagation in a heterogeneous VTI medium can be found in Carcione (1990, 1995). The anelasticity is described by the standard linear solid, also called the Zener model, which gives relaxation and creep functions in agreement with experimental results (Zener 1948).

The notation in Carcione (1995) denotes the relaxed or low-frequency limit stiffnesses with c_{IJ}, and the unrelaxed or high-frequency limit elasticities with $\hat{c}_{IJ}$. In order to use the standard notation and define the purely elastic limit in the unrelaxed regime, we denote the unrelaxed stiffnesses by c_{IJ} and the relaxed stiffnesses by c_{IJ}^0.

The 2-D velocity–stress equations for propagation in the (x,z)-plane, assigning one relaxation mechanism to dilatational anelastic deformations ($\nu=1$) and one relaxation mechanism to shear anelastic deformations ($\nu=2$), can be expressed by the following.

(1) Newton's equations:

$$\sigma_{xx,x}+\sigma_{xz,z}=\rho\dot{v}_x+f_x\,, \tag{1}$$

$$\sigma_{xz,x}+\sigma_{zz,z}=\rho\dot{v}_z+f_z\,, \tag{2}$$

where v_x and v_z are the particle velocities, σ_{xx}, σ_{zz} and σ_{xz} are the stress components, ρ is the density and f_x and f_z are the body forces. A dot above a variable denotes time differentiation.

(2) Constitutive equations:

$$\dot{\sigma}_{xx}=c_{11}v_{x,x}+c_{13}v_{z,z}+K^0\epsilon_1+2c_{55}^0\epsilon_2\,, \tag{3}$$

$$\dot{\sigma}_{zz}=c_{13}v_{x,x}+c_{33}v_{z,z}+K^0\epsilon_1-2c_{55}^0\epsilon_2\,, \tag{4}$$

$$\dot{\sigma}_{xz}=c_{55}(v_{x,z}+v_{z,x})+c_{55}^0\epsilon_3\,, \tag{5}$$

where ϵ_1, ϵ_2 and ϵ_3 are memory variables,

$$K^0=\frac{1}{2}(c_{11}^0+c_{33}^0)-c_{55}^0\,, \tag{6}$$

the relaxed stiffnesses are

$$c_{11}^0=c_{11}-D+K\eta_1+c_{55}\eta_2\,, \tag{7}$$

$$c_{33}^0=c_{33}-D+K\eta_1+c_{55}\eta_2\,, \tag{8}$$

$$c_{13}^0=c_{13}-D+K\eta_1+c_{55}(2-\eta_2)\,, \tag{9}$$

$$c_{55}^0=c_{55}\eta_2\,, \tag{10}$$

with

$$K=D-c_{55}\,,\qquad D=\frac{1}{2}(c_{11}+c_{33}) \tag{11}$$

and

$$\eta_\nu=\frac{\tau_\sigma^{(\nu)}}{\tau_\epsilon^{(\nu)}}\,, \tag{12}$$

where $\tau_\sigma^{(\nu)}$ and $\tau_\epsilon^{(\nu)}$ are material relaxation times, corresponding to dilatational ($\nu=1$) and shear ($\nu=2$) deformations.

The constitutive equations satisfy the condition that the mean stress depends only on the dilatational relaxation function in any coordinate system (the trace of the stress tensor should be invariant under coordinate transformations). Moreover, the deviatoric stresses depend solely on the shear relaxation function (Carcione 1995).

(3) Memory-variable equations:

$$\dot{\epsilon}_1=\frac{1}{\tau_\sigma^{(1)}}[(1-\eta_1^{-1})(v_{x,x}+v_{z,z})-\epsilon_1]\,, \tag{13}$$

$$\dot{\epsilon}_2=\frac{1}{2\tau_\sigma^{(2)}}[(1-\eta_2^{-1})(v_{x,x}-v_{z,z})-2\epsilon_2]\,, \tag{14}$$

$$\dot{\epsilon}_3=\frac{1}{\tau_\sigma^{(2)}}[(1-\eta_2^{-1})(v_{x,z}+v_{z,x})-\epsilon_3]\,. \tag{15}$$

FREQUENCY-DOMAIN CONSTITUTIVE EQUATION

Transforming the memory-variable equations (13), (14) and (15) to the ω-domain (e.g. $\dot{\epsilon}_1\rightarrow i\omega\epsilon_1$), and substituting the memory variables into eqs (3), (4) and (5) yields the frequency-domain constitutive equation:

$$i\omega\begin{bmatrix}\sigma_{xx}\\ \sigma_{zz}\\ \sigma_{xz}\end{bmatrix}=\begin{bmatrix}p_{11} & p_{13} & 0\\ p_{13} & p_{33} & 0\\ 0 & 0 & p_{55}\end{bmatrix}\begin{bmatrix}v_{x,x}\\ v_{z,z}\\ v_{x,z}+v_{z,x}\end{bmatrix}, \tag{16}$$

where

$$p_{11}=c_{11}-D+KM_1+c_{55}M_2\,, \tag{17}$$

$$p_{33}=c_{33}-D+KM_1+c_{55}M_2\,, \tag{18}$$

$$p_{13}=c_{13}-D+KM_1+c_{55}(2-M_2)\,, \tag{19}$$

and

$$p_{55}=c_{55}M_2 \tag{20}$$

are the complex stiffnesses, and

$$M_\nu=\eta_\nu\left(\frac{1+i\omega\tau_\epsilon^{(\nu)}}{1+i\omega\tau_\sigma^{(\nu)}}\right),\qquad \nu=1,2 \tag{21}$$

are the Zener complex moduli (Ben-Menahem & Singh 1981). Note that when $\omega\rightarrow 0$, $p_{IJ}\rightarrow c_{IJ}^0$ and that when $\omega\rightarrow\infty$, $p_{IJ}\rightarrow c_{IJ}$.

The relaxation times can be expressed as (Casula & Carcione 1992)

$$\tau_\epsilon^{(\nu)}=\frac{\tau_0}{Q_0^{(\nu)}}\left[\sqrt{Q_0^{(\nu)2}+1}+1\right] \tag{22}$$

and

$$\tau_\sigma^{(\nu)}=\frac{\tau_0}{Q_0^{(\nu)}}\left[\sqrt{Q_0^{(\nu)2}+1}-1\right], \tag{23}$$

where τ_0 is a relaxation time such that $1/\tau_0$ is the centre frequency of the relaxation peak and $Q_0^{(\nu)}$ are the minimum quality factors. Since $Q_0^{(\nu)}>0$, $\eta_\nu\leq 1$ and $c_{IJ}^0<c_{IJ}$. When $Q_0^{(\nu)}\rightarrow\infty$, $\eta_\nu\rightarrow 1$ and $c_{IJ}^0\rightarrow c_{IJ}$.

PROPAGATION CHARACTERISTICS

A general plane-wave solution for the particle velocity field $\mathbf{v}=(v_x, v_z)$ is

$$\mathbf{v}=i\omega\mathbf{U}\exp[i\omega(t-s_x x-s_z z)], \tag{24}$$

where s_x and s_z are the components of the complex slowness vector, t is the time variable and $\mathbf{U}$ is a complex vector. The real-valued slowness and attenuation vectors are given by

$$\mathbf{s}_R=[\mathrm{Re}(s_x), \mathrm{Re}(s_z)]^\top \tag{25}$$

and

$$\boldsymbol{\alpha}=-\omega[\mathrm{Im}(s_x), \mathrm{Im}(s_z)]^\top, \tag{26}$$

respectively (the symbol $\top$ denotes transpose, while Re and Im take real and imaginary parts). The complex slowness vector is then

$$\mathbf{s}=\mathbf{s}_R-i\frac{\boldsymbol{\alpha}}{\omega}, \qquad s^2=s_x^2+s_z^2. \tag{27}$$

The complex dispersion relation has the following form (Auld 1990; Carcione 1992):

$$F(s_x, s_z)=(p_{11}s_x^2+p_{55}s_z^2-\rho)(p_{33}s_z^2+p_{55}s_x^2-\rho) -(p_{13}+p_{55})^2 s_x^2 s_z^2=0, \tag{28}$$

which has two solutions corresponding to the quasi-compressional (qP) and quasi-shear (qS) waves.

Let us assume that the positive z-axis points downwards. In order to distinguish between down- and up-propagating waves, the slowness relation eq. (28) is solved for s_z, given the horizontal slowness s_x. This yields

$$s_z=\pm\frac{1}{\sqrt{2}}\left(K_1\mp\mathrm{pv}\sqrt{K_1^2-4K_2K_3}\right)^{1/2}, \tag{29}$$

where

$$K_1=\rho\left(\frac{1}{p_{55}}+\frac{1}{p_{33}}\right)+\frac{1}{p_{55}}\left[\frac{p_{13}}{p_{33}}(p_{13}+2p_{55})-p_{11}\right]s_x^2,$$

$$K_2=\frac{1}{p_{33}}(p_{11}s_x^2-\rho), \qquad K_3=s_x^2-\frac{\rho}{p_{55}},$$

and $\mathrm{pv}(z)^{1/2}$ denotes the principal value of the square root of the complex number z. The signs in s_z correspond to

(+, −) downward qP wave,

(+, +) downward qS wave,

(−, −) upward qP wave,

(−, +) upward qS wave.

The plane-wave eigenvectors belonging to a particular eigenvalue can be obtained from the qP–qS Christoffel equation (e.g. Graebner 1992):

$$\mathbf{U}=U_0\begin{pmatrix}\beta\\ \gamma\end{pmatrix}, \tag{30}$$

where U_0 is the plane-wave amplitude and

$$\beta=\mathrm{pv}\left[\frac{p_{55}s_x^2+p_{33}s_z^2-\rho}{p_{11}s_x^2+p_{33}s_z^2+p_{55}(s_x^2+s_z^2)-2\rho}\right]^{1/2} \tag{31}$$

and

$$\gamma=\pm\mathrm{pv}\left[\frac{p_{11}s_x^2+p_{55}s_z^2-\rho}{p_{11}s_x^2+p_{33}s_z^2+p_{55}(s_x^2+s_z^2)-2\rho}\right]^{1/2}. \tag{32}$$

In general, the + and − signs correspond to the qP and qS waves, respectively. However, one must choose the signs such that γ varies smoothly with the propagation angle. In the elastic case, the qP eigenvectors are orthogonal to the qS eigenvectors only when the respective slownesses are parallel. In the purely viscoelastic case, this property is not satisfied. From eqs (24), (31) and (32), and using (25) and (26), the particle velocity field can be written as

$$\mathbf{v}=i\omega U_0\begin{pmatrix}\beta\\ \gamma\end{pmatrix}\exp\{\omega[\mathrm{Im}(s_x)x+\mathrm{Im}(s_z)z]\} \times\exp\{i\omega[t-\mathrm{Re}(s_x)x-\mathrm{Re}(s_z)z]\}. \tag{33}$$

We recall that the group velocity equals the energy velocity only when there is no attenuation. Analysis of the physics requires explicit calculation of the energy velocity, since the concept of group velocity looses its physical meaning in anelastic media (Carcione 1994). The mean flux or time-average Umov–Poynting vector $\langle\mathbf{P}\rangle$ is the real part of the corresponding complex vector (Auld 1990; Carcione 1992)

$$\mathbf{P}=-\frac{1}{2}[(\sigma_{xx}v_x^*+\sigma_{xz}v_z^*)\hat{x}+(\sigma_{xz}v_x^*+\sigma_{zz}v_z^*)\hat{z}], \tag{34}$$

where the superscript * denotes a complex conjugate, and $\hat{x}$ and $\hat{z}$ are the unit vectors. Substituting the plane wave (33) and the constitutive equation (16) into eq. (34) gives

$$\mathbf{P}=\frac{1}{2}\omega^2|U_0|^2\begin{pmatrix}\beta^*X+\gamma^*W\\ \beta^*W+\gamma^*Z\end{pmatrix}\exp\{2\omega[\mathrm{Im}(s_x)x+\mathrm{Im}(s_z)z]\}, \tag{35}$$

where

$$W=p_{55}(\gamma s_x+\beta s_z), \tag{36}$$

$$X=\beta p_{11}s_x+\gamma p_{13}s_z, \tag{37}$$

and

$$Z=\beta p_{13}s_x+\gamma p_{33}s_z. \tag{38}$$

PROPERTIES OF A HOMOGENEOUS WAVE

For homogeneous waves the directions of propagation and attenuation coincide and

$$s_x=\sin\theta/V(\theta), \qquad s_z=\cos\theta/V(\theta), \tag{39}$$

where θ is the propagation angle, measured with respect to the z-axis, and $V=1/s$ is the complex velocity that can be obtained from the slowness relation (28). It yields (e.g. Carcione & Cavallini 1995)

$$\rho V^2=\frac{1}{2}(p_{55}+p_{11}\sin^2\theta+p_{33}\cos^2\theta\pm E), \tag{40}$$

with

$$E=\{[(p_{33}-p_{55})\cos^2\theta-(p_{11}-p_{55})\sin^2\theta]^2 +(p_{13}+p_{55})^2\sin^2 2\theta\}^{1/2}. \tag{41}$$

In general, the + sign corresponds to the qP wave, and the − sign to the qS wave.

For homogeneous waves,

$$\mathbf{s}=\mathrm{Re}\left(\frac{1}{V}\right)(\sin\theta,\cos\theta)^{\top}, \tag{42}$$

$$\boldsymbol{\alpha}=-\omega\,\mathrm{Im}\left(\frac{1}{V}\right)(\sin\theta,\cos\theta)^{\top} \tag{43}$$

and the quality factor is (Carcione & Cavallini 1995)

$$Q=\frac{\mathrm{Re}(V^2)}{\mathrm{Im}(V^2)}. \tag{44}$$

At the symmetry axis ($\theta=0$) and for qP waves, $V^2=\rho p_{33}$, and at the isotropy plane ($\theta=\pi/2$), $V^2=\rho p_{11}$. Then, the relation between Q factors is

$$\frac{Q(\text{symmetry axis})}{Q(\text{isotropy plane})}=\frac{c_{33}-A}{c_{11}-A},$$
$$A=D-K\,\mathrm{Re}(M_1)-G\,\mathrm{Re}(M_2). \tag{45}$$

It can be verified that $A>0$, $A<c_{11}$ and $A<c_{33}$, for most realistic materials ($A=0$ in the elastic case). This implies that whatever the ratio c_{33}/c_{11}, the ratio between Q factors is farther from unity than the elastic velocity ratio $\sqrt{c_{33}/c_{11}}$. It follows that attenuation gives a better indication of anisotropy than elastic velocity. Similarly, it can be shown that the ratio between the viscoelastic phase velocities $\mathrm{Re}(1/\sqrt{p_{11}})/\mathrm{Re}(1/\sqrt{p_{33}})$ is closer to one than the Q ratio.

Another important consequence is that, when $c_{11}>c_{33}$ (e.g. fine layering), the qP wave attenuates more along the symmetry axis than in the plane of isotropy. Note that it is not necessary to use an additional relaxation function to model Q anisotropy of the qP wave. Actually, it is the structure of the medium (described by the stiffnesses) that dictates the Q ratio between different propagation directions.

On the other hand, the quality factor of the shear wave at the symmetry axis is equal to the quality factor in the plane of isotropy, since $V^2=\rho p_{55}$ in both cases. This is realistic, since any kind of symmetry possessed by the attenuation should follow the symmetry of the crystallographic form of the material (Neumann's principle; see Nye 1987). A qS-wave anisotropy factor can be defined as the ratio of the vertical phase velocity to the phase velocity at an angle of 45° to the axis of symmetry. Again, it can be shown that, for most realistic materials, this factor is closer to one than the ratio between the respective quality factors.

REFLECTION AND REFRACTION COEFFICIENTS

The upper layer is denoted by the subscript 1 and the lower layer by the subscript 2. For clarity, the material properties of the lower medium are primed and the symbols P and S indicate the qP and qS waves, respectively. In addition, the subscripts I, R and T denote the incident, reflected and transmitted waves. Using symmetry properties to define the polarization of the reflected waves, the particle velocities for a qP wave incident from above the interface are given by

$$\mathbf{v}_1=\mathbf{v}_{P_I}+\mathbf{v}_{P_R}+\mathbf{v}_{S_R}, \tag{46}$$

$$\mathbf{v}_2=\mathbf{v}_{P_T}+\mathbf{v}_{S_T}, \tag{47}$$

where

$$\mathbf{v}_{P_I}=i\omega(\beta_{P_1},\gamma_{P_1})^{\top}\exp[i\omega(t-s_x x-s_{zP_1}z)], \tag{48}$$

$$\mathbf{v}_{P_R}=i\omega R_{PP}(\beta_{P_1},-\gamma_{P_1})^{\top}\exp[i\omega(t-s_x x+s_{zP_1}z)], \tag{49}$$

$$\mathbf{v}_{S_R}=i\omega R_{PS}(\beta_{S_1},-\gamma_{S_1})^{\top}\exp[i\omega(t-s_x x+s_{zS_1}z)], \tag{50}$$

$$\mathbf{v}_{P_T}=i\omega T_{PP}(\beta_{P_2},\gamma_{P_2})^{\top}\exp[i\omega(t-s_x x-s_{zP_2}z)], \tag{51}$$

$$\mathbf{v}_{S_T}=i\omega T_{PS}(\beta_{S_2},\gamma_{S_2})^{\top}\exp[i\omega(t-s_x x-s_{zS_2}z)]. \tag{52}$$

As in the isotropic viscoelastic case (Caviglia & Morro 1992), the boundary conditions (continuity of v and normal stress components) give Snell's law, that is, the continuity of the horizontal complex slowness s_x. The vertical slownesses s_{zP} and s_{zS}, as well as β_P, β_S, γ_P and γ_S, follow respectively the (+, −) and (+, +) sign sets given in eq. (29). The choice $U_0=1$ implies no loss of generality.

The boundary conditions require continuity of

$$v_x,\quad v_z,\quad \sigma_{zz}\quad\text{and}\quad \sigma_{xz}. \tag{53}$$

The stresses are obtained by substitution of eqs (46) and (47) into the constitutive equation (16). The boundary conditions generate the following matrix equation for the reflection and transmission coefficients:

$$\begin{pmatrix}\beta_{P_1}&\beta_{S_1}&-\beta_{P_2}&-\beta_{S_2}\\ \gamma_{P_1}&\gamma_{S_1}&\gamma_{P_2}&\gamma_{S_2}\\ Z_{P_1}&Z_{S_1}&-Z_{P_2}&-Z_{S_2}\\ W_{P_1}&W_{S_1}&W_{P_2}&W_{S_2}\end{pmatrix}\begin{pmatrix}R_{PP}\\ R_{PS}\\ T_{PP}\\ T_{PS}\end{pmatrix}=\begin{pmatrix}-\beta_{P_1}\\ \gamma_{P_1}\\ -Z_{P_1}\\ W_{P_1}\end{pmatrix}, \tag{54}$$

where W and Z are given by eqs (36) and (38), respectively.

The steps to compute the reflection and transmission coefficients are as follows.

(1) The horizontal slowness s_x is the independent parameter. It is the same for all the waves (viscoelastic Snell's law). For an incident homogeneous wave, the independent variable becomes the incidence angle θ, and s_x is obtained from eq. (39).

(2) Compute s_{zP_1}, s_{zS_1}, s_{zP_2} and s_{zS_2} from eq. (29), where the first sign is positive. For an incident homogeneous wave, s_{zP_1} can be calculated either from eq. (29) or from eq. (39).

(3) Compute β_{P_1}, β_{S_1}, β_{P_2}, β_{S_2}, γ_{P_1}, γ_{S_1}, γ_{P_2} and γ_{S_2} from eqs (31) and (32).

(4) Compute W_{P_1}, W_{S_1}, W_{P_2} and W_{S_2} from eq. (36), and Z_{P_1}, Z_{S_1}, Z_{P_2} and Z_{S_2} from eq. (38).

(5) Compute the reflection and transmission coefficients by numerically solving eq. (54).

The reflection and transmission coefficients R_{SP}, R_{SS}, T_{SP} and T_{SS} for an incident qS wave have the same scattering matrix as the qP incident wave, but the vector in the right-hand side of (54) is

$$(-\beta_{S_1},\gamma_{S_1},-Z_{S_1},W_{S_1})^{\top}. \tag{55}$$

PROPAGATION, ATTENUATION AND ENERGY DIRECTIONS

Fig. 1 illustrates the convention used to define the propagation, attenuation and energy angles. The propagation angle is perpendicular to the plane wave front. Given the components of the complex slowness vector, the propagation and attenuation

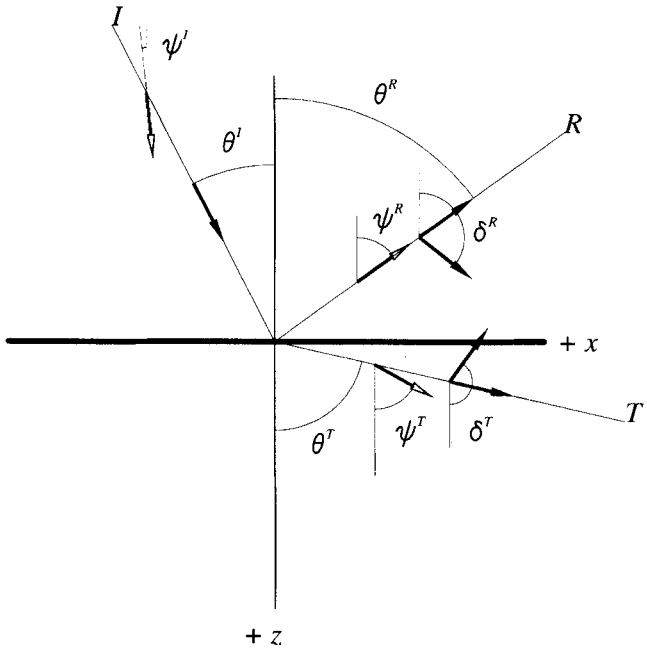

Figure 1. Figure illustrating the convention used to define the angles for the incident (I), reflected (R) and transmitted (T) waves. The angles θ, δ and ψ denote the propagation, attenuation and Umov–Poynting vector (energy) directions. The reflection angle is negative, as shown.

angles for all the waves can be obtained as

$$\tan\theta = \frac{\mathrm{Re}(s_x)}{\mathrm{Re}(s_z)}, \quad \text{and} \quad \tan\delta = \frac{\mathrm{Im}(s_x)}{\mathrm{Im}(s_z)}. \tag{56}$$

By hypothesis (see eq. 39), $\delta_{P_I} = \theta_{P_I}$, and by symmetry, $\theta_{P_R} = -\theta_{P_I}$ and $\delta_{P_R} = \theta_{P_R}$. Hence, the reflected qP wave is homogeneous.

The complex vertical slowness component of the reflected qS wave is $-s_{zS_1}$, following the $(-, +)$ sign in eq. (29). Then, the propagation and attenuation angles θ_{S_R} and δ_{S_R} are obtained from (56) with the substitution $s_z = -s_{zP_1}$. In general $\theta_{S_R} \neq \delta_{S_R}$ and the wave is inhomogeneous. Analogously, the angles of the transmitted qP wave (θ_{P_T} and δ_{P_T}) and qS wave (θ_{S_T} and δ_{S_T}) are given by (56) when $s_z = s_{zP_2}$ and $s_z = s_{zS_2}$, respectively. The transmitted waves are, in general, inhomogeneous.

The expressions of the time-averaged reflected and refracted Umov–Poynting vectors are given by eq. (35). Then, the propagation angles of the incident, reflected and refracted energy vectors are obtained from

$$\tan\psi = \frac{\mathrm{Re}(\beta^* X + \gamma^* W)}{\mathrm{Re}(\beta^* W + \gamma^* Z)}. \tag{57}$$

By symmetry we have $\psi_{P_R} = -\psi_{P_I}$.

PHASE VELOCITIES AND ATTENUATIONS

The magnitude of the phase velocities can be obtained as the reciprocal of the slownesses. From eq. (25), the phase velocity of the incident and reflected waves is simply

$$c = \{[\mathrm{Re}(s_x)]^2 + [\mathrm{Re}(s_z)]^2\}^{-1/2}. \tag{58}$$

Since the incident wave is homogeneous, use of eq. (39) yields

$$c_{P_I} = [\mathrm{Re}(V_1^{-1})]^{-1}, \tag{59}$$

where V_1 is the complex velocity for homogeneous waves in the incidence medium (see eq. 40). By symmetry, the phase velocity of the reflected qP wave c_{P_R} equals c_{P_I}.

The velocities c_{S_R}, c_{P_T} and c_{S_T} are obtained from (58) substituting s_z by s_{zS_R}, c_{zP_T} and c_{zS_T}, respectively.

The magnitude of the attenuation vectors is given by

$$\alpha = \omega\{[\mathrm{Im}(s_x)]^2 + [\mathrm{Im}(s_z)]^2\}^{-1/2}. \tag{60}$$

The incident and qP reflected waves have the same value:

$$\alpha_{P_I} = -\omega\,\mathrm{Im}(V_1^{-1}), \tag{61}$$

while the attenuations α_{S_R}, α_{P_T} and α_{S_T} are obtained from (60) substituting s_z by s_{zS_R}, c_{zP_T} and c_{zS_T}, respectively.

ENERGY FLUX BALANCE

It is well known that to balance energy flux at an interface between two isotropic single-phase media, it is necessary to consider the *interaction* energy fluxes when the media are viscoelastic (Krebes 1983). In the incidence medium, for instance, they arise from the interaction of the stress and velocity fields of the incident and reflected waves. A similar phenomenon takes place at an interface separating two porous media when the fluid viscosity is different from zero. For instance, Dutta & Ode (1983) called them *interference* fluxes and showed that they vanish for zero viscosity.

In a welded interface, the normal component of the average Umov–Poynting $\hat{z}\cdot\langle\mathbf{P}\rangle$ is continuous across the interface. This is a consequence of the boundary conditions that impose continuity of normal stresses and particle velocities. Then, using eq. (34), the balance of power flow implies the continuity of

$$-\frac{1}{2}\,\mathrm{Re}(\sigma_{xz}v_x^* + \sigma_{zz}v_z^*), \tag{62}$$

where each component is the sum of the components of the respective waves, e.g.

$$v_x = v_{xP_I} + v_{xP_R} + v_{xS_R} \tag{63}$$

in the incidence medium, and

$$\sigma_{zz} = \sigma_{zzP_T} + \sigma_{zzS_T} \tag{64}$$

in the transmission medium. Denoting by F the vertical component of the energy flux, we obtain

$$F_{P_I} + F_{P_R} + F_{S_R} + F_{P_IP_R} + F_{P_IS_R} + F_{P_RS_R} = F_{P_T} + F_{S_T} + F_{P_TS_T}, \tag{65}$$

where

$$\begin{aligned}
-2F_{P_I} &= \mathrm{Re}(\sigma_{xzP_I}v_{xP_I}^* + \sigma_{zzP_I}v_{zP_I}^*),\\
-2F_{P_R} &= \mathrm{Re}(\sigma_{xzP_R}v_{xP_R}^* + \sigma_{zzP_R}v_{zP_R}^*),\\
-2F_{S_R} &= \mathrm{Re}(\sigma_{xzS_R}v_{xS_R}^* + \sigma_{zzS_R}v_{zS_R}^*),\\
-2F_{P_IP_R} &= \mathrm{Re}(\sigma_{xzP_I}v_{xP_R}^* + \sigma_{xzP_R}v_{xP_I}^* + \sigma_{zzP_I}v_{zP_R}^* + \sigma_{zzP_R}v_{zP_I}^*),\\
-2F_{P_IS_R} &= \mathrm{Re}(\sigma_{xzP_I}v_{xS_R}^* + \sigma_{xzS_R}v_{xP_I}^* + \sigma_{zzP_I}v_{zS_R}^* + \sigma_{zzS_R}v_{zP_I}^*),\\
-2F_{P_RS_R} &= \mathrm{Re}(\sigma_{xzP_R}v_{xS_R}^* + \sigma_{xzS_R}v_{xP_R}^* + \sigma_{zzP_R}v_{zS_R}^* + \sigma_{zzS_R}v_{zP_R}^*),\\
-2F_{P_T} &= \mathrm{Re}(\sigma_{xzP_T}v_{xP_T}^* + \sigma_{zzP_T}v_{zP_T}^*),\\
-2F_{S_T} &= \mathrm{Re}(\sigma_{xzS_T}v_{xS_T}^* + \sigma_{zzS_T}v_{zS_T}^*),\\
-2F_{P_TS_T} &= \mathrm{Re}(\sigma_{xzP_T}v_{xS_T}^* + \sigma_{xzS_T}v_{xP_T}^* + \sigma_{zzP_T}v_{zS_T}^* + \sigma_{zzS_T}v_{zP_T}^*).
\end{aligned} \tag{66}$$

For instance, F_{P_I} is the energy flux of the incident qP wave and $F_{P_I P_R}$ is the interference flux between the incident and reflected qP waves. In the elastic limit, it can be shown that the interference fluxes vanish. Further algebra implies that the fluxes given in the preceding equation are proportional to the real parts of

$$
\begin{aligned}
&F_{P_I} \rightarrow \beta^*_{P_1} W_{P_1} + \gamma^*_{P_1} Z_{P_1}\,,\\
&F_{P_R} \rightarrow -(\beta^*_{P_1} W_{P_1} + \gamma^*_{P_1} Z_{P_1})|R_{PP}|^2\,,\\
&F_{S_R} \rightarrow -(\beta^*_{S_1} W_{S_1} + \gamma^*_{S_1} Z_{S_1})|R_{PS}|^2\,,\\
&F_{P_I P_R} \rightarrow -2i(\beta^*_{P_1} W_{P_1} - \gamma^*_{P_1} Z_{P_1})\,\mathrm{Im}(R_{PP})\,,\\
&F_{P_I S_R} \rightarrow (\beta^*_{S_1} W_{P_1} - \gamma^*_{S_1} Z_{P_1}) R^*_{PS} - (\beta^*_{P_1} W_{S_1} - \gamma^*_{P_1} Z_{S_1}) R_{PS}\,,\\
&F_{P_R S_R} \rightarrow -[(\beta^*_{S_1} W_{P_1} + \gamma^*_{S_1} Z_{P_1}) R_{PP} R^*_{PS}\\
&\qquad + (\beta^*_{P_1} W_{S_1} + \gamma^*_{P_1} Z_{S_1}) R^*_{PP} R_{PS}]\,,\\
&F_{P_T} \rightarrow (\beta^*_{P_2} W_{P_2} + \gamma^*_{P_2} Z_{P_2})|T_{PP}|^2\,,\\
&F_{S_T} \rightarrow (\beta^*_{S_2} W_{S_2} + \gamma^*_{S_2} Z_{S_2})|T_{PS}|^2\,,\\
&F_{P_T S_T} \rightarrow (\beta^*_{S_2} W_{P_2} + \gamma^*_{S_2} Z_{P_2}) T_{PP} T^*_{PS} + (\beta^*_{P_2} W_{S_2} + \gamma^*_{P_2} Z_{S_2}) T^*_{PP} T_{PS}\,,
\end{aligned}
\tag{67}
$$

where the proportionality factor is $(1/2)\omega^2$.

We define the energy reflection and transmission coefficients as

$$
\begin{aligned}
&ER_{PP} = \left(\frac{F_{P_R}}{F_{P_I}}\right)^{1/2}, \qquad ER_{PS} = \left(\frac{F_{S_R}}{F_{P_I}}\right)^{1/2},\\
&ET_{PP} = \left(\frac{F_{P_T}}{F_{P_I}}\right)^{1/2}, \qquad ET_{PS} = \left(\frac{F_{S_T}}{F_{P_I}}\right)^{1/2},
\end{aligned}
\tag{68}
$$

and the interference coefficients as

$$
\begin{aligned}
&I_{P_I P_R} = \frac{F_{P_I P_R}}{F_{P_I}}, \qquad I_{P_I S_R} = \frac{F_{P_I S_R}}{F_{P_I}},\\
&I_{P_R S_R} = \frac{F_{P_R S_R}}{F_{P_I}}, \qquad I_{P_T S_T} = \frac{F_{P_T S_T}}{F_{P_I}},
\end{aligned}
\tag{69}
$$

to obtain the following energy flux balance equation:

$$
1 + ER^2_{PP} + ER^2_{PS} + I_{P_I P_R} + I_{P_I S_R} + I_{P_R S_R} = ET^2_{PP} + ET^2_{PS} + I_{P_T S_T}\,.
\tag{70}
$$

We have chosen the square root of the energy ratio (Gutenberg 1944) since it is more nearly related to the response given in terms of particle velocities and displacements.

UMOV–POYNTING THEOREM, ENERGY VELOCITIES AND QUALITY FACTORS

The energy-balance equation or Umov–Poynting theorem for the propagation of time-harmonic fields in anisotropic viscoelastic media is given in Carcione & Cavallini (1993). For inhomogeneous viscoelastic plane waves it is

$$
-2\boldsymbol{a}^{\top}\cdot\mathbf{P} = 2i\omega[\langle\epsilon_s\rangle - \langle\epsilon_v\rangle] - \omega\langle\epsilon_d\rangle\,,
\tag{71}
$$

where $\langle\epsilon_s\rangle$ and $\langle\epsilon_v\rangle$ are the time-averaged strain and kinetic energy densities, respectively, and $\langle\epsilon_d\rangle$ is the time-averaged dissipated energy density. The dot denotes the scalar product.

The energy velocity $\mathbf{v}_e$ is defined as the ratio of the average power-flow density $\langle\mathbf{P}\rangle$ to the mean energy density $\langle\epsilon\rangle = \langle\epsilon_s + \epsilon_v\rangle$. Fortunately, it is not necessary to calculate the strain and kinetic energies explicitely, since, as shown by Carcione & Cavallini (1993),

$$
\langle\epsilon\rangle = \mathbf{s}_R\cdot\langle\mathbf{P}\rangle\,.
\tag{72}
$$

Then, the energy velocity can be calculated as

$$
\mathbf{v}_e = \frac{\langle\mathbf{P}\rangle}{\mathbf{s}_R\cdot\langle\mathbf{P}\rangle}\,.
\tag{73}
$$

Using eqs (25) and (35), the energy velocity is

$$
\mathbf{v}_e = \frac{\mathrm{Re}(\beta^* X + \gamma^* W)\hat{x} + \mathrm{Re}(\beta^* W + \gamma^* Z)\hat{z}}{\mathrm{Re}(s_x)\,\mathrm{Re}(\beta^* X + \gamma^* W) + \mathrm{Re}(s_z)\,\mathrm{Re}(\beta^* W + \gamma^* Z)}\,,
\tag{74}
$$

which by (57) becomes

$$
\mathbf{v}_e = [\mathrm{Re}(s_x + s_z\cot\psi)]^{-1}\hat{x} + [\mathrm{Re}(s_x\tan\psi + s_z)]^{-1}\hat{z}\,.
\tag{75}
$$

An alternative expression for the energy velocity is obtained from the fact that, as in the elastic case, the phase velocity is the projection of the energy velocity onto the propagation direction. This relation was demonstrated by Carcione & Cavallini (1993) for inhomogeneous waves propagating in a general anisotropic viscoelastic medium. Thus, we have

$$
v_e = c/\cos(\psi - \theta)\,.
\tag{76}
$$

In terms of the tangents defined in eqs (56) and (57), the magnitude of the energy velocity is

$$
v_e = \frac{[(1+\tan^2\psi)(1+\tan^2\theta)]^{1/2}}{(1+\tan\psi\tan\theta)}\,c\,.
\tag{77}
$$

The quality factor, defining the attenuation in terms of energy, is twice the ratio of the average strain-energy density and the average dissipated energy density:

$$
Q = \frac{2\langle\epsilon_s\rangle}{\langle\epsilon_d\rangle}\,.
\tag{78}
$$

The quality factor of the incident homogeneous wave is simply (Carcione & Cavallini 1995)

$$
Q_{P_I} = \frac{\mathrm{Re}(V_I^2)}{\mathrm{Im}(V_I^2)}\,.
\tag{79}
$$

For the reflected and refracted waves we make use of the following fundamental relations derived by Carcione & Cavallini (1993):

$$
\langle\epsilon_d\rangle = \frac{2}{\omega}\boldsymbol{a}^{\top}\cdot\langle\mathbf{P}\rangle
\tag{80}
$$

and

$$
\langle\epsilon_s\rangle = \frac{1}{2}\,\mathrm{Re}(\mathbf{s}^*\cdot\mathbf{P})\,.
\tag{81}
$$

Substitution of these relations into eq. (79) and use of eq. (25) yields

$$
Q = -\frac{\mathrm{Re}(\mathbf{s}^*\cdot\mathbf{P})}{2\,\mathrm{Im}(\mathbf{s})\cdot\langle\mathbf{P}\rangle}\,,
\tag{82}
$$

or, using eq. (35),

$$Q=-\frac{\mathrm{Re}[(\beta^* X+\gamma^* W)s_x^*+(\beta^* W+\gamma^* Z)s_z^*)]}{2[\mathrm{Re}(\beta^* X+\gamma^* W)\,\mathrm{Im}(s_x)+\mathrm{Re}(\beta^* W+\gamma^* Z)\,\mathrm{Im}(s_z)]}\,. \tag{83}$$

EXAMPLE

In this section we consider a particular example and compare the results with that of the purely elastic case, that is, both media elastic. To begin, we briefly consider the following two special cases. If the incidence medium is elastic and the transmission medium anelastic, the theory imposes that the attenuation vectors of the transmitted waves are perpendicular to the interface. On the other hand, if the incidence medium is anelastic and the transmission medium is elastic, the transmitted waves are inhomogeneous of the *elastic type*, that is, the angle between the Umov–Poynting vector and the attenuation vector is $\pi/2$. The demonstration for *SH* waves can be found in Carcione (1997) and the interpretation, for the isotropic case, is given by Krebes & Slawinsky (1991).

The elastic or unrelaxed stiffnesses of the incidence medium are given by

$$c_{11}=\rho V_P^2(\pi/2)\,,\qquad c_{33}=\rho V_P^2(0)\,,$$

$$c_{55}=\rho V_S^2\,,\qquad c_{13}=3.906\ \mathrm{GPa}\,,$$

where

$$V_P(\pi/2)=2.79\ \mathrm{km\ s^{-1}}\,,\qquad V_P(0)=2.24\ \mathrm{km\ s^{-1}}\,,$$

$$V_S=1.01\ \mathrm{km\ s^{-1}}\,,\qquad \rho=2700\ \mathrm{kg\ m^{-3}}\,.$$

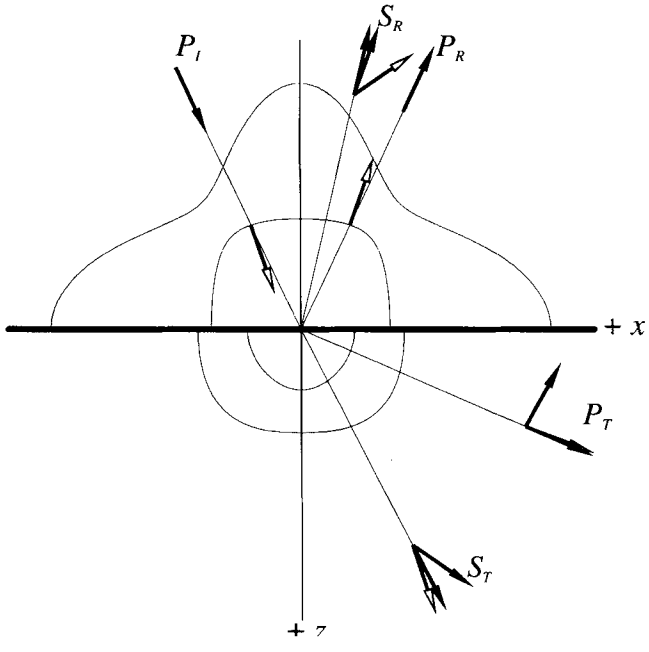

Figure 2. Reflection (P_R and S_R) and transmitted (P_T and S_T) plane waves for an incident *P* wave with $\theta_{P_I}=25°$. The slowness curves (for homogeneous waves) of the upper and lower medium are represented, with the inner curves corresponding to the quasi-compressional waves. The lines coincide with the propagation direction, and the convention for the attenuation and energy vectors is that indicated in Fig. 1.

It is assumed that the medium has two relaxation peaks centred at f_0 = 12.625 Hz ($\tau_0=1/2\pi f_0$), with minimum quality factors of $Q_0^{(1)}$ = 20 and $Q_0^{(2)}$ = 15, corresponding to dilatational and shear deformations, respectively.

On the other hand, the unrelaxed properties of the transmission medium are

$$c'_{11}=\rho' V_P'^2(\pi/2)\,,\qquad c'_{33}=\rho' V_P'^2(0)\,,$$

$$c'_{55}=\rho' V_S'^2\,,\qquad c'_{13}=28.72\ \mathrm{GPa}\,,$$

where

$$V'_P(\pi/2)=4.6\ \mathrm{km\ s^{-1}}\,,\qquad V'_P(0)=4.1\ \mathrm{km\ s^{-1}}\,,$$

$$V'_S=2.4\ \mathrm{km\ s^{-1}}\,,\qquad \rho'=3200\ \mathrm{kg\ m^{-3}}\,.$$

As before, there are two relaxation peaks centred at the same frequency, with $Q_0^{(1)}=60$ and $Q_0^{(2)}=35$.

The slowness curves for homogeneous waves are shown in Fig. 2, where the inner curve corresponds to the *qP* wave. The figure also shows the attributes of the incident, reflected and transmitted waves for an incidence angle $\theta_{P_I}=25°$. In the anelastic case, the Umov–Poynting vectors (non-solid arrows) of the incident and reflected *qP* waves are almost perpendicular to the slowness surface. Actually, the orthogonality property

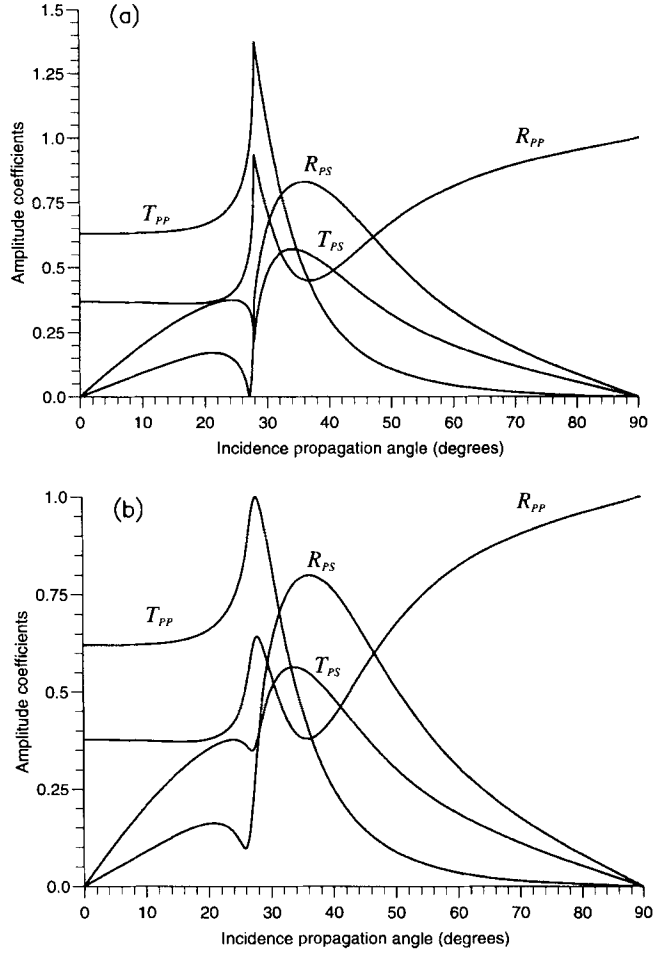

Figure 3. Absolute values of the amplitude reflection and transmitted coefficients versus incidence propagation angle corresponding to the elastic (a) and viscoelastic (b) cases.

is only verified in the elastic case (Carcione 1994). The transmitted waves show a high degree of inhomogeneity (that is, the propagation and attenuation vectors do not have the same direction), in particular the qP wave, whose attenuation vector is almost perpendicular to the direction of the energy vector.

Fig. 3 shows the absolute value of the amplitude coefficients versus the incidence propagation angle for the elastic (a) and viscoelastic (b) cases. If the two media are elastic, there is a critical angle at approximately 27°, which occurs when the Umov–Poynting vector of the refracted qP wave becomes parallel to the interface. If the lower medium is anelastic or both media are anelastic, the energy vector of the refracted qP wave points downwards for all the incidence propagation angles. Thus, there is no critical angle. This can be seen in Fig. 4, where the absolute values of the energy coefficients are displayed as a function of θ_{P_I} (a) and ψ_{P_I} (b). Since ET_{PP} is always greater than zero, the P_T Umov–Poynting vector is never parallel to the interface.

The propagation, energy and attenuation angles, as a function of the incidence angle, are shown in Fig. 5. By symmetry, the propagation and energy angles of the reflected P_R wave are equal to θ_{P_I} and ψ_{P_I}, respectively. For viscoelastic plane waves travelling in an anisotropic medium, $|\theta-\delta|$ may exceed 90°

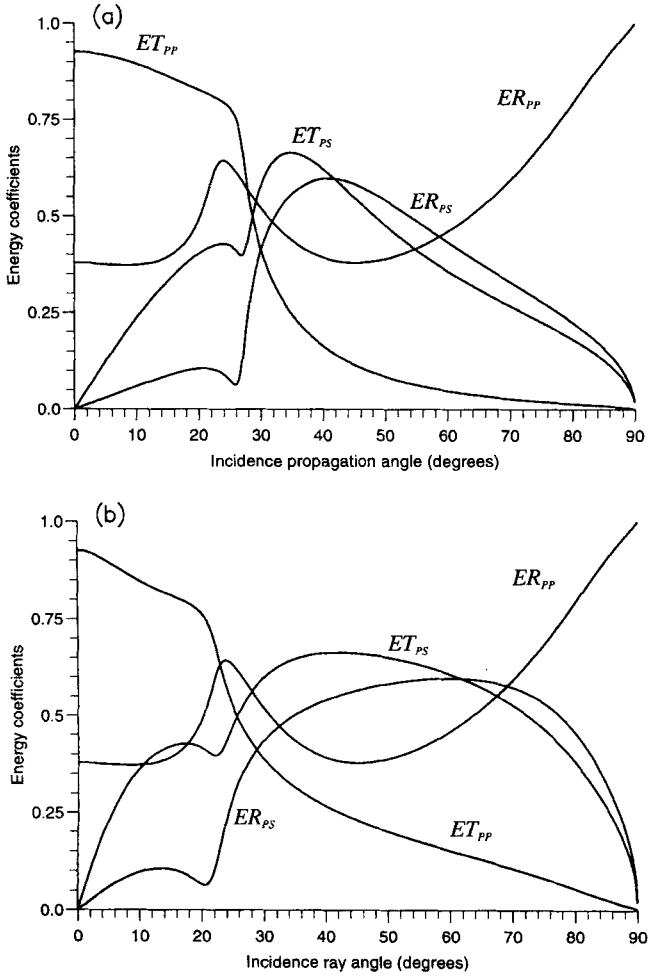

Figure 4. Absolute values of the energy reflection and transmitted coefficients versus incidence propagation angle (a) and ray (energy) angle (b) corresponding to the viscoelastic case.

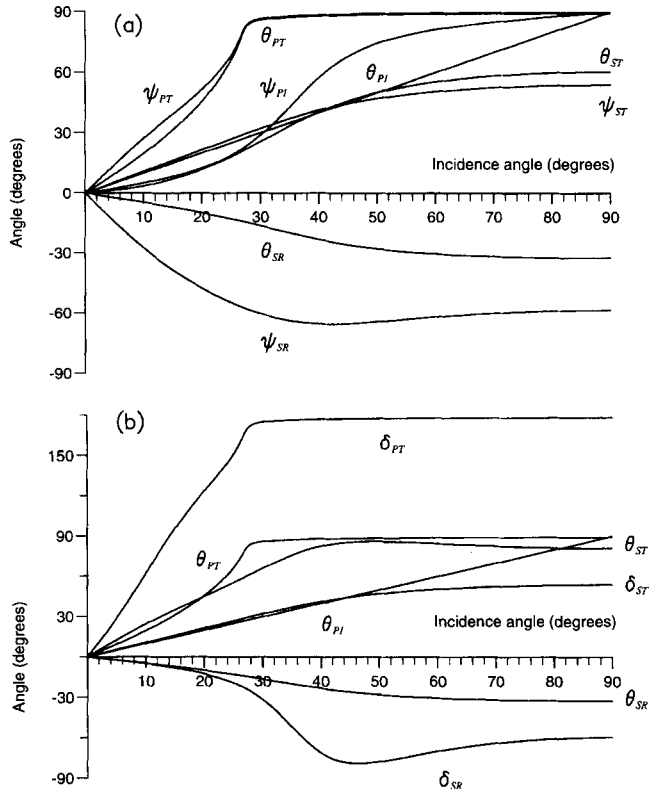

Figure 5. Energy (a) and attenuation (b) angles versus incidence angle for the incident, reflected and refracted waves. The propagation angle is also shown in both cases.

(Carcione 1997). However, the difference $|\psi-\delta|$ must be less than 90°. Indeed, since the energy loss is always positive, eq. (80) implies that the magnitude of the angle between $\boldsymbol{a}$ and $\langle\mathbf{P}\rangle$ is always strictly less than $\pi/2$. This property is verified in Fig. 5. Moreover, this figure shows that, at approximately the elastic critical angle and beyond, the P_T energy angle is close to $\pi/2$ and that the attenuation vector is almost perpendicular to the interface. This indicates that, practically, the transmitted qP wave behaves as an evanescent wave of the elastic type beyond the (elastic) critical angle. Fig. 6 displays the phase shifts versus the incidence propagation angle, indicating that there are substantial differences between the elastic (a) and the anelastic (b) cases.

The phase velocities are shown in Fig. 7. They depend on the propagation direction mostly because the media are anisotropic but, to a lesser extent, also because of their viscoelastic inhomogeneous character. Despite the fact that there is no critical angle, the phase velocity of the transmitted qP wave shows a similar behaviour (in qualitative terms) to the elastic phase velocity. Beyond the elastic critical angle, the velocity is mainly governed by the value of the horizontal slowness, and finally approaches the phase velocity of the incidence wave. The attenuation curves (see Fig. 8) show that dissipation of the S_R and P_T waves is very anisotropic. In particular the P_T attenuation is very high after the elastic critical angle, due to the evanescent character of the wave.

Fig. 9 shows the energy velocity of the different waves. The difference between energy and phase velocities is due solely to the anisotropy, since they coincide in isotropic media (Carcione 1994). The quality factors are shown in Fig. 10.

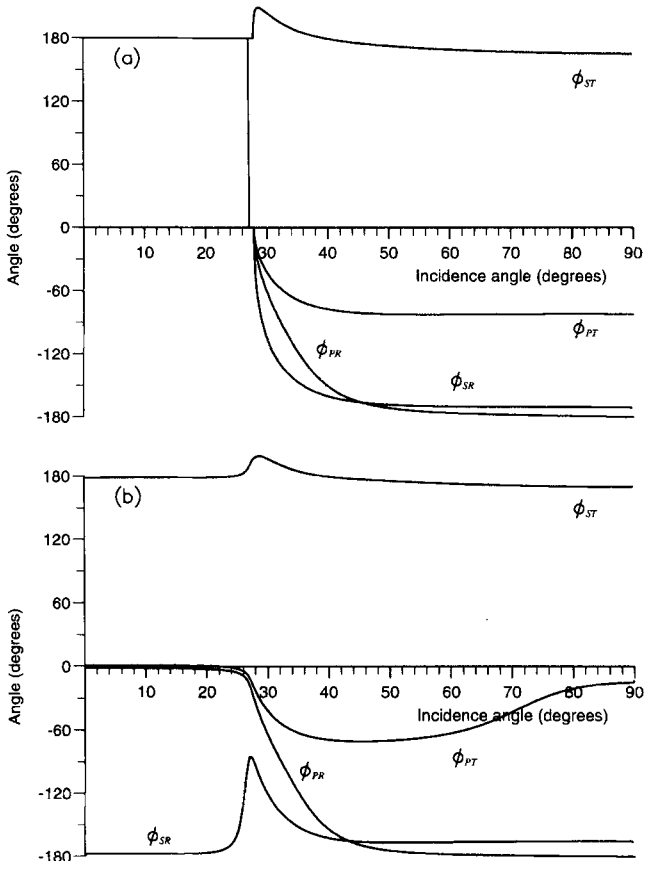

Figure 6. Phase angles versus incidence propagation angle for the incident, reflected and refracted waves corresponding to the elastic (a) and viscoelastic (b) cases.

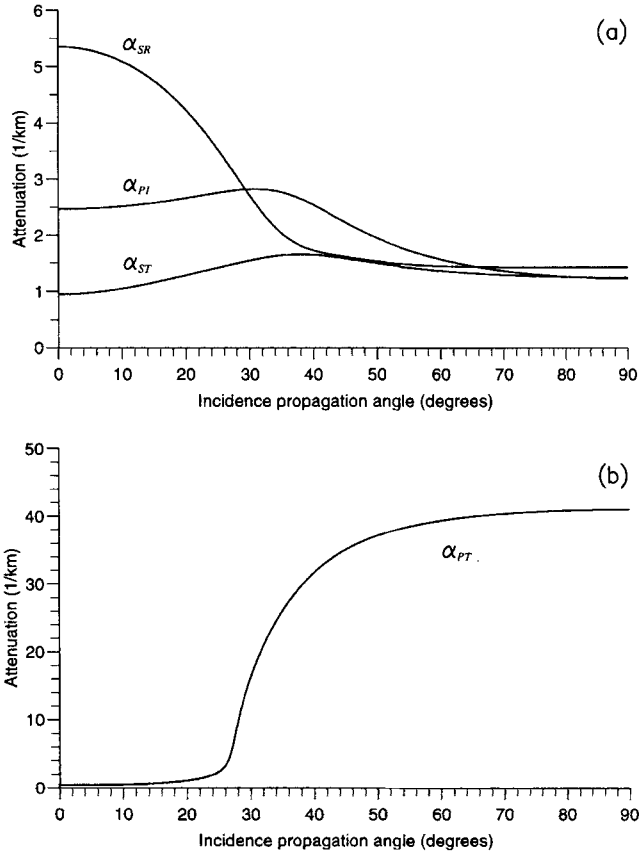

Figure 8. Attenuations of the incident, reflected and refracted waves versus the incidence propagation angle. (b) corresponds to the transmitted quasi-compressional wave.

Before the critical angle, the highest quality factor is that of the P_T wave, in agreement with its attenuation curve shown in Fig. 8(b). However, beyond that angle, the quality factor seems to contradict the attenuation curve of the other waves: the very strong attenuation is not reflected in the quality factor. This apparent paradox means that the usual relation $\alpha \approx \omega s_R / 2Q$ (e.g. Carcione & Cavallini 1995) is not valid for evanescent-type waves travelling closer to interfaces, even if $Q \gg 1$. Finally, Fig. 11 shows the square root of the interference coefficients versus the incidence propagation angle. It indicates that much of the energy is lost by interference between the different waves beyond the elastic critical angle. The interference between the P_T and S_T waves is particularly high, and is comparable to ET_{PP} around 30° incidence. Note that these coefficients vanish in the purely elastic case.

A numerical simulation of the reflection–transmission problem was carried out using a wave-modelling algorithm

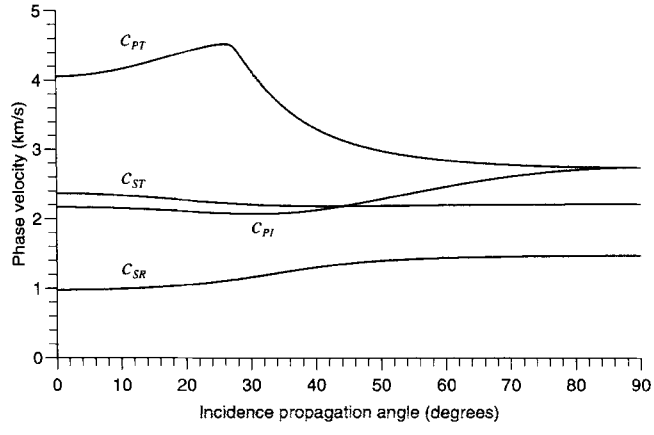

Figure 7. Phase velocities of the incident, reflected and refracted waves versus the incidence propagation angle for the viscoelastic case.

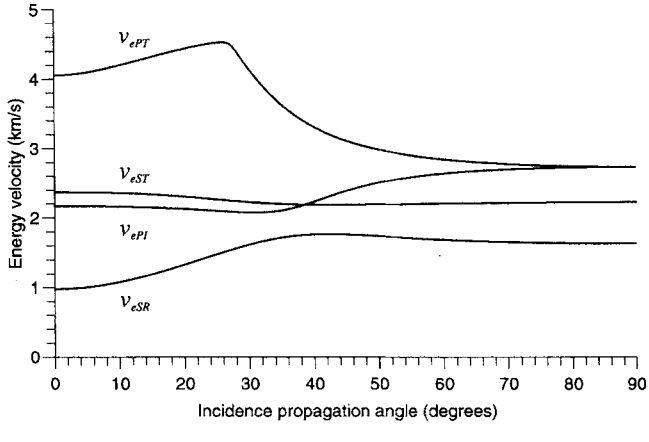

Figure 9. Energy velocities of the incident, reflected and refracted waves versus the incidence propagation angle for the viscoelastic case.

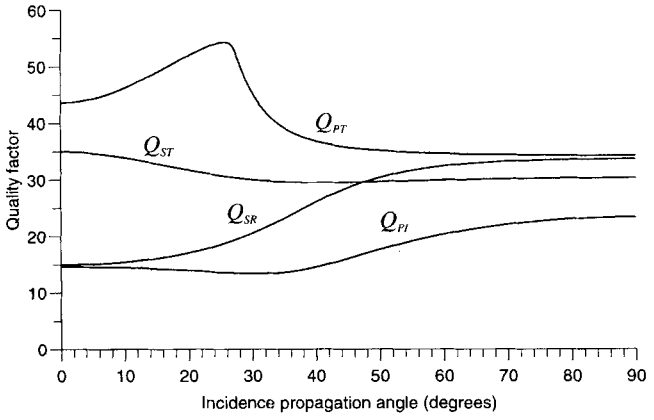

Figure 10. Quality factors of the incident, reflected and refracted waves versus the incidence propagation angle for the viscoelastic case.

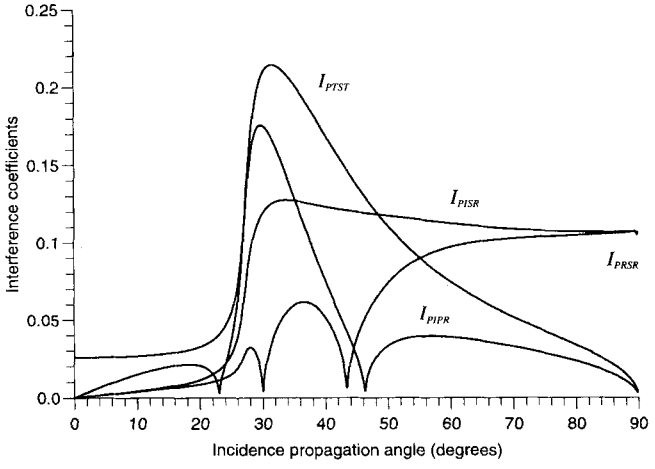

Figure 11. Square root of the interference coefficients versus the incidence propagation angle.

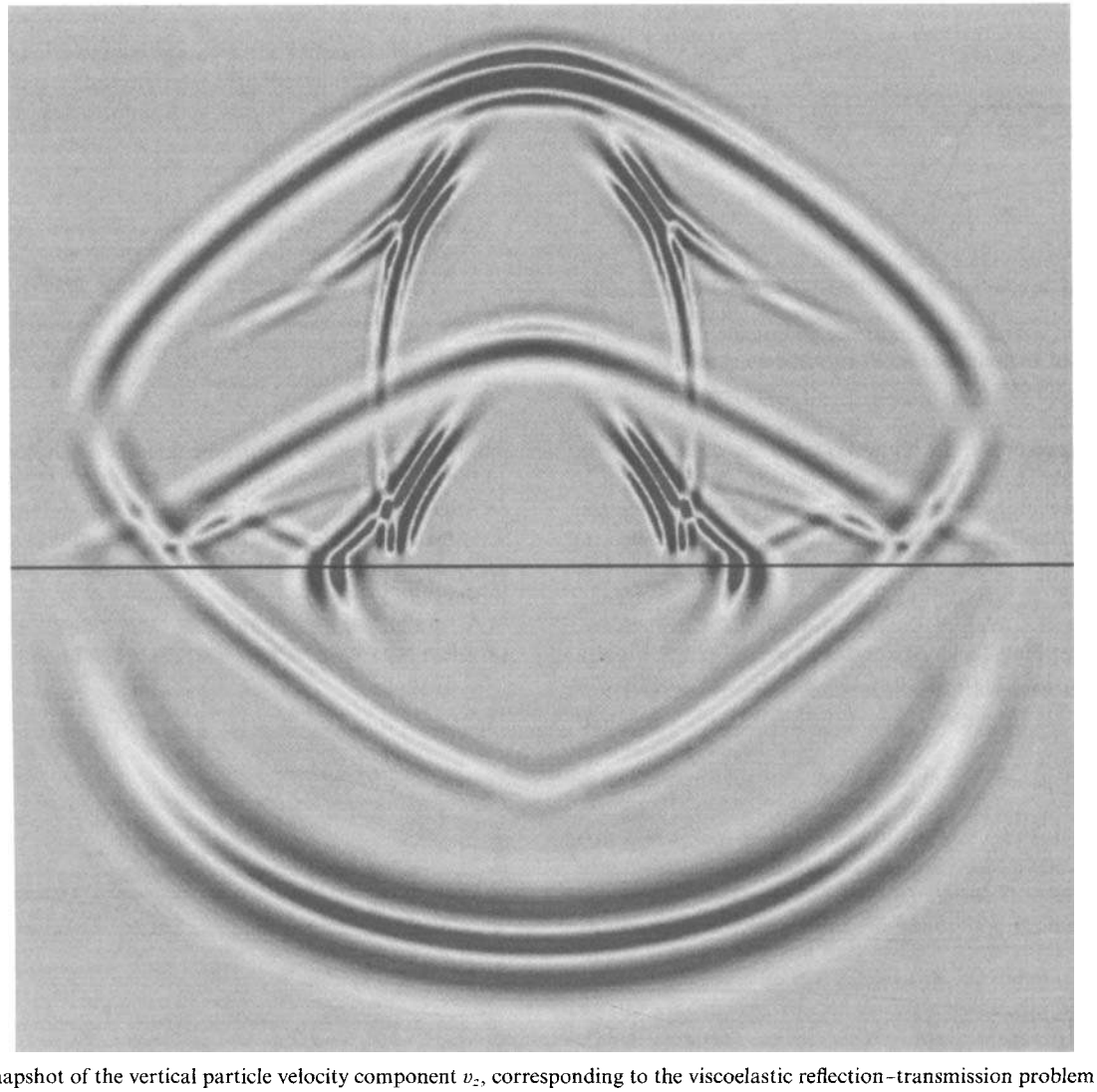

Figure 12. Snapshot of the vertical particle velocity component v_z, corresponding to the viscoelastic reflection–transmission problem at 800 ms.

based on the Fourier pseudospectral method to compute the spatial derivatives, and a fourth-order Runge–Kutta technique to compute the wavefield recursively in time (see Carcione 1995). The numerical mesh has 231×231 points with a grid spacing $D_X = D_Z = 20$ m. The source is a Ricker-type wavelet located at 600 m above the interface, and has a dominant frequency of 12.625 Hz, that is, the central frequency of the relaxation peaks. In order to generate mainly qP energy, the

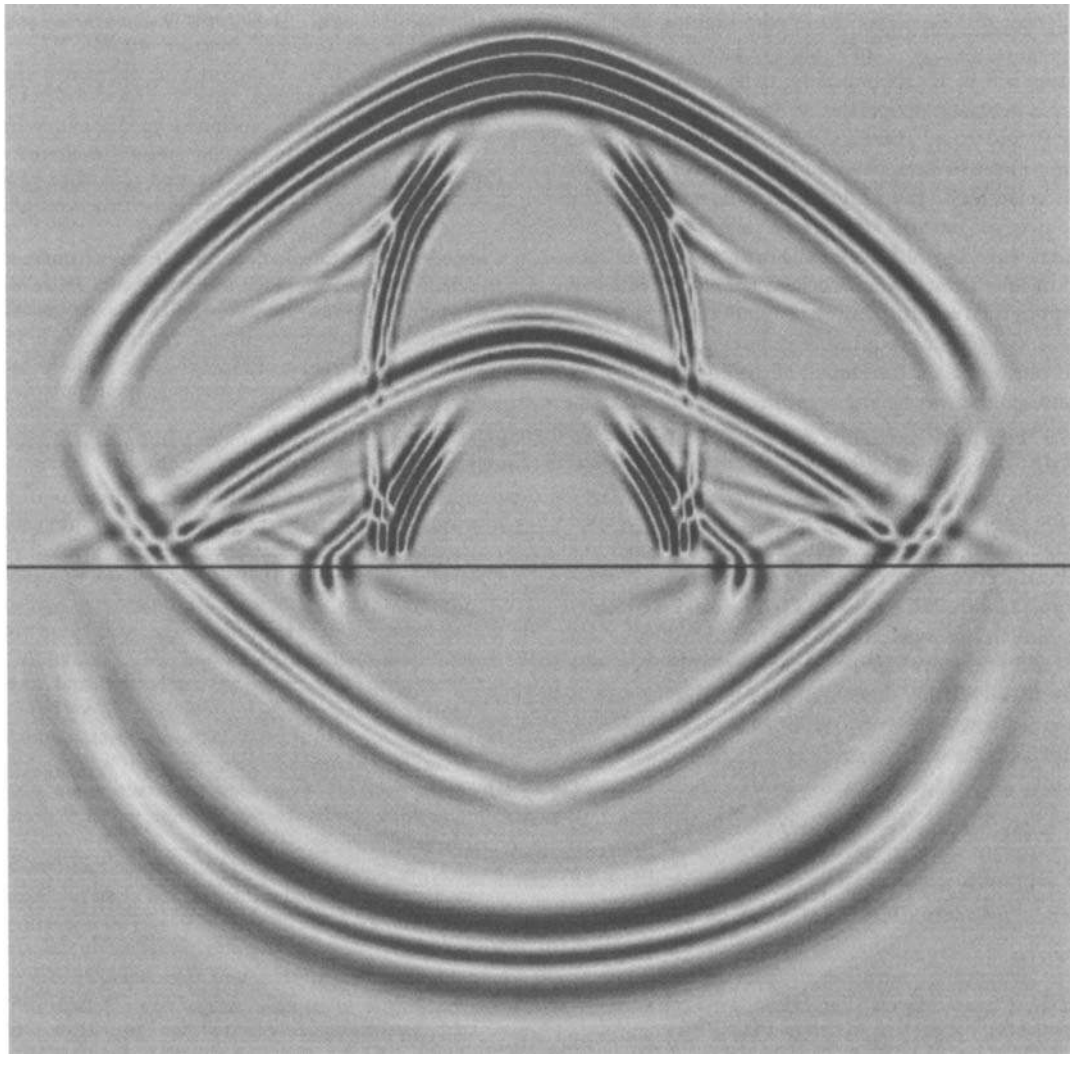

Figure 13. Snapshot of the vertical particle velocity component v_z, corresponding to the elastic reflection–transmission problem at 800 ms.

source is a discrete delta function, equally distributed in the stress components σ_{xx} and σ_{zz} (a mean stress perturbation). Fig. 12 shows a snapshot at 800 ms, which covers the incidence ray angles from 0° to approximately 62°.

In the upper medium, the primary waves are the qP wave followed by the qS wave, which shows high-amplitude cuspidal triangles despite the dilatational nature of the source. Moreover, the P_R and S_R are travelling upwards, away from the interface. Near the centre of the mesh the events are mainly related to the reflection of the cuspidal triangles. In the lower medium, the P_T wave is followed by the S_T wave, which resembles a continuation of the incident qP wave, since both events have similar velocities (see Fig. 2). In principle, Fig. 12 should be interpreted by comparison with Fig. 4(b). However, Fig. 12 displays the vertical particle velocity v_z, and Fig. 4(b) the square root of the normal power flow. Moreover, the interpretation must take into account that the source has a non-isotropic radiation pattern, and that the incidence wave is also affected by anisotropic attenuation effects. Despite these facts, a qualitative interpretation can be attempted. First, the amplitudes of the S_R and S_T waves are very low at normal incidence, as predicted by the ER_{PS} and ET_{PS} curves, respectively. In particular, the amplitude of the S_T wave increases for increasing ray angle, in agreement with ET_{PS}. Also in good agreement is the amplitude variation of the P_T wave compared with the ET_{PP} curve. Another event is the planar wavefront connecting the reflected and transmitted qP waves. This is a conical or head wave that cannot be entirely explained by the plane-wave analysis. Despite the fact that a critical angle does not exist, since ψ_{PT} never reaches $\pi/2$ (see Fig. 5a), some of the P_T energy disturbs the interface, giving rise to the conical wave. This problem deserves further research. For illustration, the snapshot corresponding to the purely elastic case is shown in Fig. 13. The maximum amplitude in this figure is approximately three times the maximum amplitude in Fig. 12. As can be appreciated, for example in the primary qP wave, the wave fronts travel with a faster velocity than the viscoelastic wave fronts, due to the choice of the elastic case in the unrelaxed limit.

CONCLUSIONS

We have investigated the reflection–transmission problem in viscoelastic transversely isotropic media. From a plane analysis we have obtained the attributes of the reflected and transmitted waves, such as the energy reflection coefficients,

the phase and energy velocities, the quality factor and the interference coefficients. A particular example allows a detailed investigation of the phenomena caused by the combined anisotropic anelastic properties of the media and waves. In the purely elastic case, there is a critical angle for the refracted quasi-compressional wave. In the anelastic case, this angle does not exist, since the Umov–Poynting vector of the refracted wave is never parallel to the interface. However, the behaviour of that wave beyond the elastic critical angle is very similar to that of an elastic evanescent wave. Their effects can be seen in the numerical experiment, through the generation of a conical wave in the upper medium. A remarkable difference from the purely elastic case is that much of the energy is lost by interference between the waves. For some incidence angles, the interference coefficients can have the same magnitude as the reflection and transmission coefficients. Another important result is that the usual simple relation between quality factor and attenuation cannot be applied to the inhomogeneous viscoelastic plane waves generated at the interface.

The present study considered an incident homogeneous wave. Therefore, additional research is necessary to study the effects of the inhomogeneity of the incident wave on the reflection and transmission coefficients. Moreover, the presence of strong anisotropy and symmetry axes not perpendicular to the interface, combined with the anelastic effects, also deserves further research.

ACKNOWLEDGMENTS

This work was supported in part by Norsk Hydro a.s. (Bergen).

REFERENCES

Auld, B.A., 1990. *Acoustic Fields and Waves in Solids,* Vol. 1, Robert E. Krieger Publishing Co., Malabar, FL.

Ben-Menahem, A. & Singh, S.J., 1981. *Seismic Waves and Sources,* Springer-Verlag, Berlin.

Borcherdt, R.D., Glassmoyer, G. & Wennerberg, L., 1986. Influence of welded boundaries in anelastic media on energy flow, and characteristics of *P*, *S*-I and *S*-II waves: observational evidence for inhomogeneous body waves in low-loss solids, *J. geophys. Res.*, **91,** 11 503–11 118.

Buchen, 1971. Plane waves in linear viscoelastic media, *Geophys. J. R. astr. Soc.*, **23,** 531–542.

Carcione, J.M., 1990. Wave propagation in anisotropic linear viscoelastic media: theory and simulated wavefields, *Geophys. J. Int.*, **101,** 739–750. Erratum: 1992, **111,** 191.

Carcione, J.M., 1992. Anisotropic Q and velocity dispersion of finely layered media, *Geophys. Prospect.*, **40,** 761–783.

Carcione, J.M., 1994. Wavefronts in dissipative anisotropic media, *Geophysics,* **59,** 644–657.

Carcione, J.M., 1995. Constitutive model and wave equations for linear, viscoelastic, anisotropic media, *Geophysics,* **60,** 537–548.

Carcione, J.M., 1997. Reflection and refraction of anti-plane shear waves at a plane boundary between viscoelastic anisotropic media, *Proc. R. Soc. Lond.,* A, in press.

Carcione, J.M. & Cavallini, F., 1993. Energy balance and fundamental relations in anisotropic-viscoelastic media, *Wave Motion,* **18,** 11–20.

Carcione, J.M. & Cavallini, F., 1995. Attenuation and quality factor surfaces in anisotropic-viscoelastic media, *Mech. Mat.*, **19,** 311–327.

Casula, G. & Carcione, J.M., 1992. Generalized mechanical model analogies of linear viscoelastic behaviour, *Boll. Geofis. Teor. Appl.*, **34,** 235–256.

Caviglia, G. & Morro, A., 1992. *Inhomogeneous Waves in Solids and Fluids,* World Scientific, Singapore.

Cooper, H.F., 1967. Reflection and transmission of oblique plane waves at a plane interface between viscoelastic media, *J. acoust. Soc. Am.*, **42,** 1064–1069.

Daley, P.F. & Hron, F., 1977. Reflection and transmission coefficients for transversely isotropic media, *Bull. seism. Soc. Am.*, **67,** 661–675.

Dutta, N.C. & Ode, H., 1983. Seismic reflections from a gas–water contact, *Geophysics,* **48,** 14–32.

Graebner, M., 1992. Plane-wave reflection and transmission coefficients for a transversely isotropic solid, *Geophysics,* **57,** 1512–1519.

Gutenberg, B., 1944. Energy ratio of reflected and refracted seismic waves, *Bull. seism. Soc. Am.*, **34,** 85–102.

Henneke, E.G., 1971. Reflection–refraction of a stress wave at a plane boundary between anisotropic media, *J. acoust. Soc. Am.*, **51,** 210–217.

Keith C.M. & Crampin, S., 1977. Seismic body waves in anisotropic media: reflection and refraction at a plane interface, *Geophys. J. R. astr. Soc.*, **49,** 181–208.

Krebes, E.S., 1983. The viscoelastic reflection/transmission problem: two special cases, *Bull. seism. Soc. Am.*, **73,** 1673–1683.

Krebes, E.S. & Slawinski, M.A., 1991. On raytracing in an elastic–anelastic medium, *Bull. seism. Soc. Am.*, **81,** 667–686.

Musgrave, M.J.P., 1960. Reflection and refraction of plane elastic waves at a plane boundary between aeolotropic media, *Geophys. J. R. astr. Soc.*, **3,** 406–418.

Nye, J.F., 1987. *Physical Properties of Crystals—Their Representation by Tensors and Matrices,* Clarendon Press, Oxford.

Rokhlin, S.I., Bolland, T.K. & Adler, L., 1986. Reflection–refraction of elastic waves on a plane interface between two generally anisotropic media, *J. acoust. Soc. Am.*, **79,** 906–918.

Schoenberg, M., 1971. Transmission and reflection of plane waves at an elastic-viscoelastic interface, *Geophys. J. R. astr. Soc.*, **25,** 35–47.

Zener, C., 1948. *Elasticity and Anelasticity of Metals,* University of Chicago Press, IL.